

NOTICE CONCERNING COPYRIGHT RESTRICTIONS

This document may contain copyrighted materials. These materials have been made available for use in research, teaching, and private study, but may not be used for any commercial purpose. Users may not otherwise copy, reproduce, retransmit, distribute, publish, commercially exploit or otherwise transfer any material.

The copyright law of the United States (Title 17, United States Code) governs the making of photocopies or other reproductions of copyrighted material.

Under certain conditions specified in the law, libraries and archives are authorized to furnish a photocopy or other reproduction. One of these specific conditions is that the photocopy or reproduction is not to be "used for any purpose other than private study, scholarship, or research." If a user makes a request for, or later uses, a photocopy or reproduction for purposes in excess of "fair use," that user may be liable for copyright infringement.

This institution reserves the right to refuse to accept a copying order if, in its judgment, fulfillment of the order would involve violation of copyright law.

DETERMINATION OF FRACTURE APERTURE
A MULTI-TRACER APPROACH

Charles E. Fox and Roland N. Horne

Stanford University, Dept. of Petroleum Eng., 350 Mitchell Bldg., Stanford CA 94305

ABSTRACT

This work shows that fracture aperture can be calculated from tracer tests involving two tracers with different affinities for adsorption onto the rock. In 1983 Jensen proved that fissure width can be determined when adsorptive effects are neglected. Adsorption introduces an additional unknown, the retardation factor, into the governing equations. When two tracers are injected, the number of available equations expands to match the number of unknowns.

This article also presents equations based on the matrix diffusion model which allow estimation of fracture aperture through visual examination of tracer tests. Tracer data from tests in the Wairakei geothermal field in New Zealand were analyzed by the visual method. The results were compared to computations using nonlinear regression. The two analyses differed randomly with an average variation of ± 40%.

INTRODUCTION

The disposal of produced water is an important part of geothermal development. Often the water contains pollutants which preclude dumping into the biosphere. Re injection of waste fluids into the productive formation is normally the most economical solution. Injection programs can have positive effects such as pressure maintenance and the replacement of reservoir fluid. Conversely the introduction of cooled fluids may damage the productivity of the reservoir. Cold water could flow into production wells and decrease thermal recovery.

Geothermal fields are especially prone to breakthrough problems because the primary flow paths are through fractures. Cooled fluids can short circuit the low permeability matrix and flow quickly through the fissures from the injector to the producer. The prediction of the arrival of the cold front is therefore of considerable economic importance.

The process of heat transfer between fluids and heat sources has been extensively studied. Solutions are readily available for the flow of fluids through heat exchangers of almost any configuration. The major problem for the geothermal engineer is to define the geometry of the system since the other parameters such as heat transfer coefficients are known.

Recently the matrix diffusion model has been developed to describe the flow of tracers or contaminants through fractured porous media. The use of this model is extended in this report to cover the determination of fracture aperture from tracer tests in which adsorption is significant. Once this parameters is known the estimation of thermal breakthrough is straight forward.

THEORY

As stated in the introduction, many authors have utilized the matrix diffusion model to study the flow of tracers through fractures. Contributions of this work include the derivation of a fracture aperture equation and the coupling of the matrix diffusion model to chromatographic analysis.

Derivation of the Governing Equations

The two governing equations are expressions of material balance. Figures 1 and 2 show the control volumes used to develop the fracture flow and matrix diffusion governing equations. The fracture and adjoining matrix are assumed to be homogeneous and isotropic. Convection, diffusion and adsorption occur within the system, and while longitudinal dispersion terms are not included, Taylor Dispersion is used to describe diffusion within the fracture itself (Taylor 1953). Taylor Dispersion holds that diffusion in the direction of flow is negligible in relation to the velocity of flow but is quick enough so that there is no concentration gradient across the small width of the fracture. While the effective diffusivity is used throughout this report, Neretnieks (1980) presents an excellent survey of the various diffusion constants used in other literature. Adsorption is modeled as linear, instantaneous reaction (mass adsorbed is proportional to the concentration).

Fracture Flow Governing Equation

The fracture flow equation describes the transport of a tracer through a fissure. Figure 1 depicts a fracture with a width, *b*, a height, *h*, and a differential length, *dx*. A tracer of concentration *C_f* is transported through the fracture with a velocity, *v*. Fick's Law of diffusion describes the flux of tracer which flows through the fracture wall. Tracer is also lost from the fracture due to adsorption which is characterized as a linear function of concentration. *K_a*, the areal partition coefficient, models the equilibrium between the mass of tracer adsorbed onto the fracture wall and the concentration of the tracer in the fracture.

Placing the terms shown in Figure 1 into a mass balance equation:

$$Mass\ Entering - Mass\ Leaving = Mass\ Accumulating \quad (1)$$

$$v b h C_f - v b h \left(C_f + \frac{\partial C_f}{\partial x} dx \right) + 2 h dx D_e \frac{\partial C_f}{\partial y} \Big|_{y=0} - 2 h dx K_a \frac{\partial C_f}{\partial t} = h b dx \frac{\partial C_f}{\partial t} \quad (2)$$

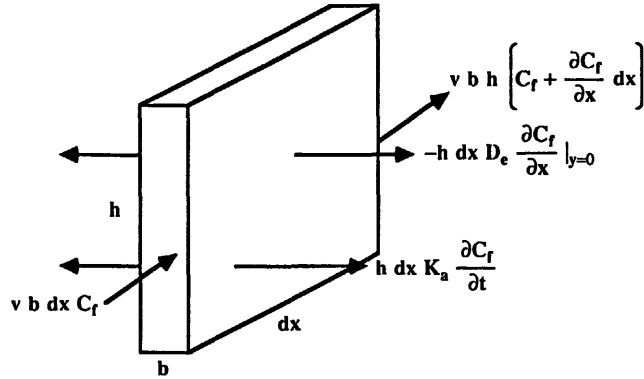


Figure 1: Fracture Flow

Dividing both sides of the equation by $hbdx$ yields:

$$-v \frac{\partial C_f}{\partial x} + \frac{2}{b} D_e \frac{\partial C_f}{\partial y} \Big|_{y=0} - \frac{2}{b} K_a \frac{\partial C_f}{\partial t} = \frac{\partial C_f}{\partial t} \quad (3)$$

Note that h dropped out of the equation.

Rearranging Equation 3:

$$\left(1 + \frac{2}{b} K_a\right) \frac{\partial C_f}{\partial t} = \frac{2}{b} D_e \frac{\partial C_f}{\partial y} \Big|_{y=0} - v \frac{\partial C_f}{\partial x} \quad (4)$$

The retardation factor, R_D , is defined to be $(1 + \frac{2}{b} K_a)$ (Freeze and Cherry 1979), hence:

$$R_D \frac{\partial C_f}{\partial t} = \frac{2}{b} D_e \frac{\partial C_f}{\partial y} \Big|_{y=0} - v \frac{\partial C_f}{\partial x} \quad (5)$$

This article will refer to both Equations 4 and 5 as the fracture flow governing equation.

Matrix Diffusion Governing Equation

The matrix diffusion equation describes the transport of tracer through the porous matrix. Figure 2 depicts an elemental volume representing the matrix. Fick's Second Law of Diffusion models the diffusion of tracer through the rock where C_p denotes the concentration in the pores of the matrix (mass per volume of liquid). Mass accumulates in the volume due to adsorption onto the rock grains.

Placing the terms shown in Figure 2 into a mass balance equation:

$$Mass_{Entering} - Mass_{Leaving} = Mass_{Accumulating} \quad (6)$$

$$-(hdx)D_e \frac{\partial C_p}{\partial y} - [-(hdx)D_e \left(\frac{\partial C_p}{\partial y} + \frac{\partial^2 C_p}{\partial y^2} dy\right)] = (hdx dy) \frac{\partial C_m}{\partial t} \quad (7)$$

C_m is the concentration within a given volume of rock (mass per volume of liquid and solid).

Dividing both sides of the equation by $(hdx)dy$ yields:

$$D_e \frac{\partial^2 C_p}{\partial y^2} = \frac{\partial C_m}{\partial t} \quad (8)$$

Again h divides out of the equation. h does not appear in either governing equation. The solution will not depend on the fracture height.

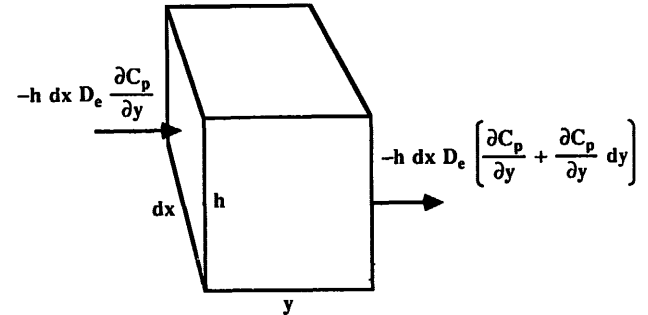


Figure 2: Matrix Diffusion

The mass in the matrix, C_m (mass per bulk volume), is comprised of free solute in the pores, C_p (mass per pore volume), and adsorbed mass on the grains S (mass per bulk volume).

$$C_m = \phi C_p + S \quad (9)$$

For small concentrations a linear isotherm may be used to model the partitioning between the rock and fluid. K_v (pore volume per bulk volume) is the volumetric partition coefficient. K_v is related to K_a by the surface area to volume ratio of the rock.

$$S = K_v C_p \quad (10)$$

Substituting Equation 10 into Equation 9

$$C_m = (\phi + K_v) C_p \quad (11)$$

Equations 8 and 11 may be combined:

$$(\phi + K_v) \frac{\partial C_p}{\partial t} = D_e \frac{\partial^2 C_p}{\partial y^2} \quad (12)$$

Some authors define $(\phi + K_v)$ as the volumetric equilibrium constant, $K_d \rho_p$ and utilize the apparent diffusivity, D_a where $D_a = D_e / K_d \rho_p$ (Neretnieks 1980). Equation 13 is the matrix diffusion governing equation.

$$\frac{\partial C_p}{\partial t} = \frac{D_e}{\phi + K_v} \frac{\partial^2 C_p}{\partial y^2} \quad (13)$$

Solution

The governing equations may be solved for a step change at the inlet (Figure 3) where there is no tracer present prior to injection (Carslaw and Jaeger 1959). The equations were nondimensionalized by using six dimensionless groups. Concentration was nondimensionalized by dividing by the injection or reference concentration ($C_D = C/C_0$). The lengths were divided by the distance between the inlet and outlet ($x_D = x/L$ etc.). The retardation factor, R_D , is the same as previously defined. K_D is the dimensionless partition coefficient where $K_D = \phi + K_v$.

Two groups were defined using an unknown time, t^* . t^* defines the length of the fracture divided by the velocity of flow (L/v). This is the time for a tracer to travel from an injector to a producer where there is no adsorption or diffusion. It is the breakthrough time for a nonsorbing tracer. The dimensionless time and dimensionless diffusivity are defined as follows: $t_D = t/t^*$; $D_D = D_e t^* / L^2$.

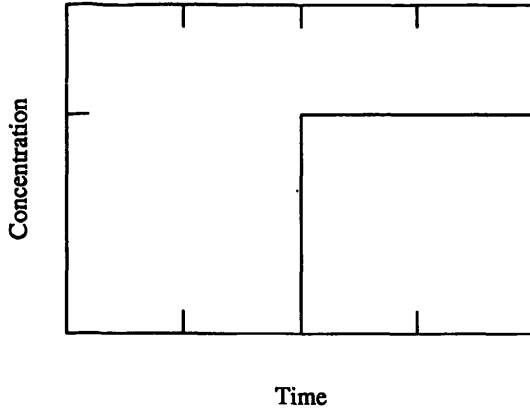


Figure 3: Inlet Condition - Step Change

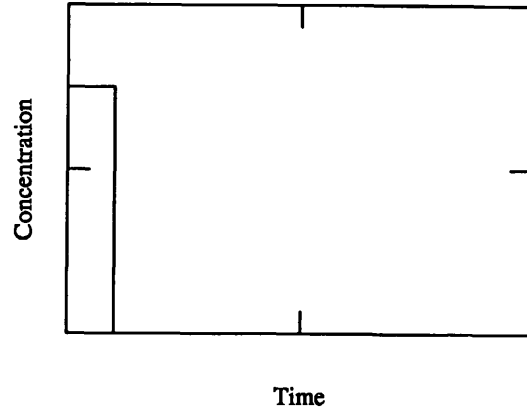


Figure 5: Inlet Condition - Pulsed Injection

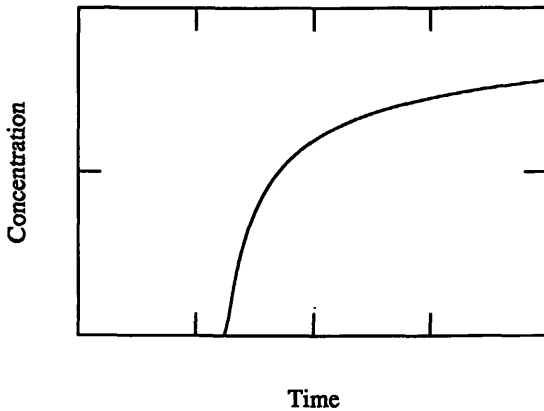


Figure 4: Outlet Response to Step Change

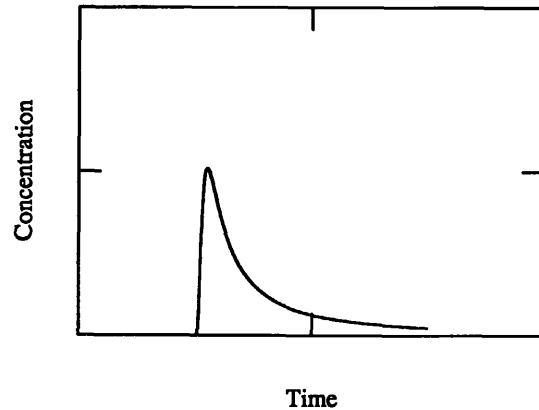


Figure 6: Outlet Response to Pulsed Injection

The solution to the step input is given in Equation 14. Notice that the retardation factor is buried with the dimensionless time inside a square root. The retardation factor does not affect the shape of the response. It simply translates the profile forward or backward in time. Also at the outlet or producing well, $x = L$ or $x_D = 1$; therefore, the solution does not depend of the fracture length. Figure 4 shows the response to a step input.

$$C_{fD} = \text{erfc} \left[\frac{x_D(D_D K_D)^{1/2}}{b_D(t_D - x_D R_D)^{1/2}} \right]; \text{ for } t_D > R_D \quad (14)$$

$$C_{fD} = 0; \text{ for } t_D \leq x_D R_D \quad (15)$$

Fracture Aperture Equation

Most field tests do not usually involve simple step changes at the inlet. Instead, tracers are more commonly injected over a short period of time. When a tracer is injected into an injection well for a time, Δt (Figure 5), the response will be as shown in Figure 6. This boundary condition can be handled by superposition of the step change solution (Equation 14). Equation 16 is the derivative of the solution to this input condition.

$$C'_{fD} = A_D \left\{ \frac{\exp \left[\frac{-D_D K_D x_D^2}{b_D^2 (t_D - R_D)} \right]}{(t_D - x_D R_D)^{3/2}} - \frac{\exp \left[\frac{-D_D K_D x_D^2}{b_D^2 (t_D - \Delta t - R_D)} \right]}{(t_D - \Delta t - x_D R_D)^{3/2}} \right\} \quad (16)$$

$$\text{for } t_D - \Delta t > x_D R_D$$

$$\text{where } A_D = \frac{x_D(D_D K_D)^{1/2}}{\sqrt{\pi} b_D (t_D - x_D R_D)^{3/2}}$$

At the peak of the tracer recovery curve, the derivative of the concentration with respect to time is zero. By setting Equation 16 to zero and rearranging the result in dimensional form, one can derive the fracture aperture equation (Equation 17). Equation 17 relates the fracture aperture to t^* and several other parameters. The other parameters can be determined through logs or laboratory tests on cores. The fracture aperture appears on both sides of the equation and an iterative solution is required.

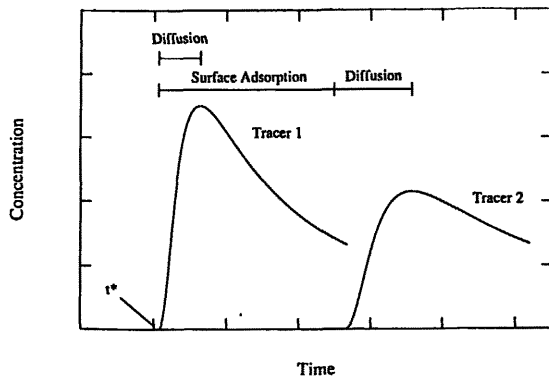


Figure 7: Chromatographic Effects of Diffusion and Adsorption

Fracture Aperture Equation

$$b^2 = \frac{D_e(\phi + K_v)t^{*2}\Delta t}{(t_p - R_D t^*)(t_p - \Delta t - R_D t^*) \ln \left[1 - \frac{\Delta t}{t_p - R_D t^*} \right]^{-3/2}} \quad (17)$$

where $R_D = 1 + \frac{2}{b}K_a$

For no adsorption ($K_a = K_v = 0$):

$$b^2 = \frac{D_e\phi t^{*2}\Delta t}{(t_p - t^*)(t_p - \Delta t - t^*) \ln \left[1 - \frac{\Delta t}{t_p - R_D t^*} \right]^{-3/2}} \quad (18)$$

For an instantaneous or spike injection, Δt approaches zero. This is the normal boundary condition for injection of a radioactive tracer. Equation 19 is the fracture aperture equation for instantaneous injection. This expression provides a noniterative solution.

Fracture Aperture Equation - Instantaneous Injection

$$b = \frac{K_a t^* + \sqrt{K_a^2 t^{*2} + 6D_e(\phi + K_v)(t_p - t^*)t^{*2}}}{3(t_p - t^*)} \quad (19)$$

For no adsorption ($K_a = K_v = 0$):

$$b = t^* \sqrt{\frac{2D_e\phi}{3(t_p - t^*)}} \quad (20)$$

Inferring values of b from the fracture aperture equation requires the injection of either one nonsorbing or two dissimilar adsorbing tracers. Either method will allow estimation of t^* . This parameter appears in every form of the aperture equation and must be determined before the fracture width can be estimated. When a nonsorbing tracer is injected, the breakthrough time corresponds to t^* , and the aperture can be calculated in a straightforward manner. t^* cannot be determined directly when dealing with a sorbing tracer because adsorption causes a retardation of the tracer movement. When one sorbing tracer is utilized, two unknowns, b and t^* , appear in the one equation. If two tracers with different affinities for adsorption are injected, one can write the fracture aperture equation twice

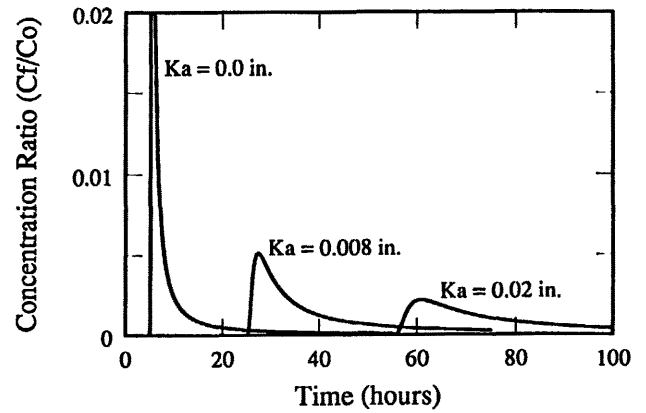


Figure 8: Synthetic Tracer Breakthrough Curves

— once for each tracer. With two equations, the two unknowns can both be calculated. Although the evaluation is simpler when using a nonsorbing tracer, it is important to note that truly nonsorbing tracers are uncommon. Skagius, Svedberg and Neretnieks (1982) have noted the adsorption of radioactive elements on minerals.

In many cases adsorption is the major cause for delaying the peak returns from t^* . Adsorption will dominate the slower diffusion process. Remember that surface adsorption will translate the entire profile while diffusion will simply separate the breakthrough and peak times. Figure 7 illustrates this point. Tracer 1 is a nonsorbing tracer; therefore, the breakthrough time and t^* are identical. Diffusion causes the small difference between t^* and t_p . Tracer 2 is an adsorbing tracer in which adsorptive effects cause a translation. This translation is the major reason that t^* and the peak time are different. Notice the relatively small diffusional effects. For the case where adsorptive effects dominate:

$$t_p - \Delta t - R_D t^* \approx 0 \quad (21)$$

Substituting for R_D and solving for b yields the:

Approximate Fracture Aperture Equation

$$b \approx \frac{2K_a t^*}{t_p - \Delta t - t^*} \quad (22)$$

Note the great dependence on K_a . This is unfortunate because K_a is the most difficult parameter to measure.

Analysis of Synthetic Tracer Tests

Synthetic tracer tests were generated using the matrix diffusion model. They are analyzed in this section to illustrate the utility of the fracture aperture equation.

Figure 8 shows breakthrough tracer returns for three tracers. The flow is through a fracture of 0.004 inches in width. Tracer 1 is nonsorbing. Tracer 2 has an areal partition coefficient of twice the aperture. Tracer 3's areal partition coefficient is five times the width. The input data are summarized in Tables 1 and 2.

It is a simple matter to analyze the nonsorbing tracer test. The breakthrough and peak times are determined from the graph. Along with these parameters, the diffusivity, porosity and injection time are plugged into Equation 18. Note that the breakthrough time for the nonsorbing tracer is equal to t^* (5 hr = 1000 ft/200 ft/hr).

Fracture Data	
<i>b</i>	0.004 in.
<i>x</i>	1000 ft
<i>h</i>	100 ft
<i>v</i>	200 ft/hr
Matrix Data	
ϕ	2 %
D_e	$1.86 \cdot 10^{-6}$ ft ² /hr

Table 1: Synthetic Tracer Test – Formation Data

Tracer Data		
Tracer 1	Tracer 2	Tracer 3
K_v 0.000	K_v 0.500	K_v 1.000
K_a 0.000 in	K_a 0.008 in.	K_a 0.020 in.
Injection Interval		
Δt	5 min	

Table 2: Synthetic Tracer Test – Injection Data

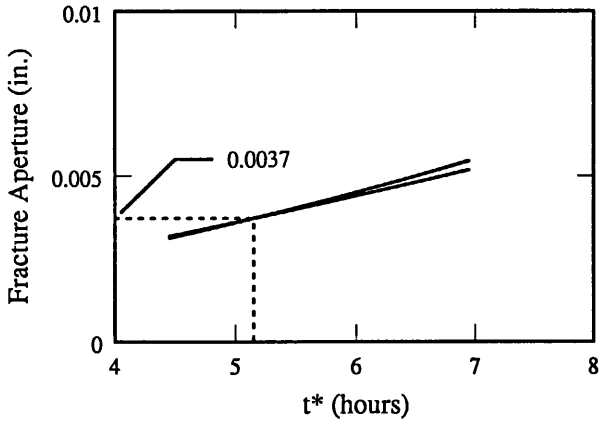


Figure 9: Fracture Aperture Cross Plot – Approximate Equation

When analyzing adsorbing tracers, two tracers are necessary. Figure 9 presents a cross plot of t^* vs. fracture aperture for tracers 2 and 3. The approximate equation (22) was used to generate these curves. There is little separation between the two curves; highlighting the sensitivity of the solution to K_a . The lines cross at 5.15 hrs and 0.0037 in. while the input parameters were 5 hours and 0.004 in. If the iterative equation were used (Figure 10), the solution would be exact (excluding round off error). Figure 11 compares the two solutions.

ANALYSIS OF WAIRAKEI FIELD DATA

This section describes the analysis of tracer tests from the Wairakei Geothermal Field in New Zealand. The results compare favorably to those of an investigation by Jensen (1983). While he also used the matrix diffusion model, his analysis was done using a nonlinear regression program.

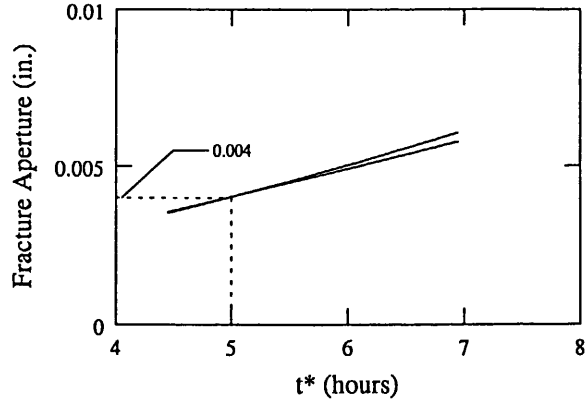


Figure 10: Fracture Aperture Cross Plot – Iterative Solution

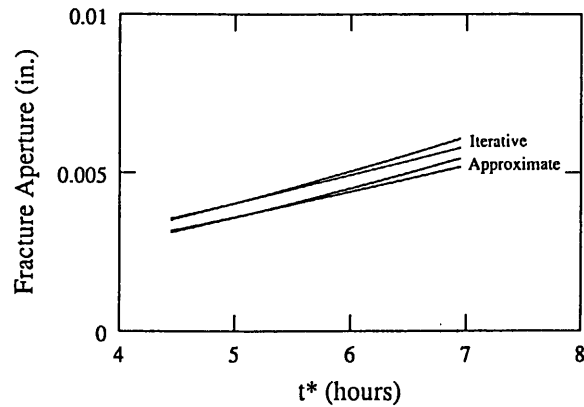


Figure 11: Approximate vs. Iterative Solution

Geology

Wairakei is one of New Zealand's larger geothermal resources. The field lies in a large thermal area, 200 miles north of Wellington on the North Island. The primary production comes from the interface between the Waiora and Wairakei formations, and the primarily flow paths are through fissures. The major faults, the Kaiapo, Wairakei and Waiora, all strike northeast to southwest and are intersected by minor faults inside the productive area (Figure 12). Jensen (1983) provides a fairly complete synopsis of the geology. For a more complete description see Grindley (1965).

Tracer Tests

Two tracer injection tests are analyzed in this report. They were performed by the Institute of Nuclear Sciences, Department of Scientific and Industrial Research, New Zealand. In March 1979, 155 GBq of iodine-131 were injected into well WK107 at 1096 feet (Figure 12). A vial containing the tracer was shattered inside a surface by-pass connection thus producing an instantaneous injection (McCabe, Barry and Manning 1983). Radioactivity was subsequently seen in ten wells. Later in June, 165 GBq were injected into well WK101 at 1312 feet, and sensors detected the iodide in twelve wells. Some wells did not show significant response and were not analyzed by Jensen (1983).

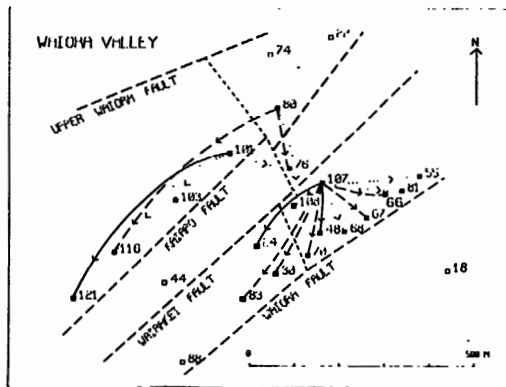


Figure 12: Well Locations in Wairakei Field (from McCabe *et al.* 1983)

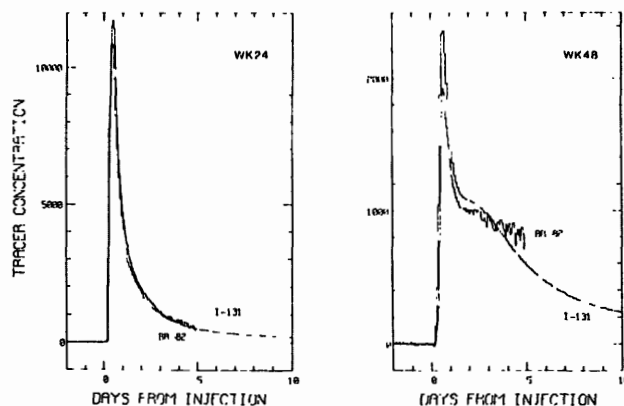


Figure 13: Chromatographic Movement of Iodide and Bromide – Wairakei (from McCabe *et al.* 1983)

Analysis and Comparison

The data could only be analyzed if an adsorption isotherm were assumed. A literature survey produced no publications regarding the sorption of iodide on the minerals found in the Wairakei field although the chromatographic performance of iodide vs. bromide was tested in Wairakei (Figure 13). There was no difference in the arrival times or shapes of the breakthrough curves (McCabe 1983). The responses may have been alike either because neither tracer adsorbed, or both adsorbed similarly. The similarity is probable since both iodide and bromide are halogens. A factor which tended to reduce the affinity of iodide for the rock was its electrical potential. Anions have little attraction for identically charged formations; however, they are known to adsorb onto the crystal edges of otherwise negatively charged clays (Gray and Darley 1980). In the absence of better information the best assumption was that iodide does not adsorb.

Equation 20, valid for a nonsorbing tracer, was used to analyze the data. Only four parameters were needed: porosity, diffusivity, breakthrough time and time to peak concentration. The two times were found by inspecting the concentration vs. time plots, and the porosity was estimated by logs and core analysis. The diffusivity could have been inferred from the porosity (Perkins and Johnston 1963) or measured directly. To facilitate comparison with Jensen's calculations, this analysis assumed a porosity of 1% and a diffusivity of $4.32 \cdot 10^{-6} \text{ ft}^2/\text{day}$ ($5 \cdot 10^{-7} \text{ cm}^2/\text{s}$).

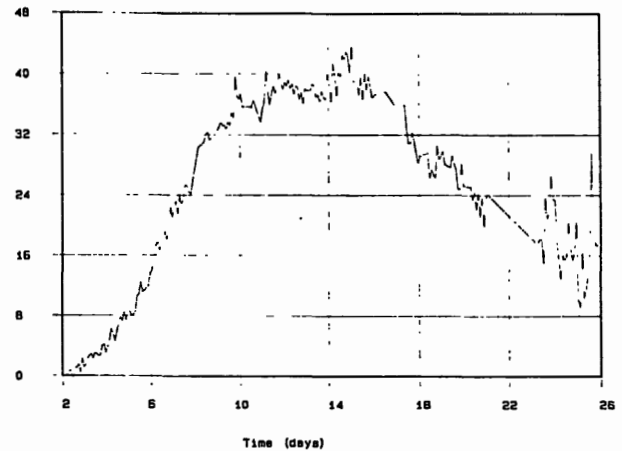


Figure 14: WK68 Tracer Breakthrough Curve from CWK107

From Perkins and Johnston (1963):

$$D_e = \frac{D_0}{F\phi} \tag{23}$$

For a carbonate or consolidated formation:

$$F = \frac{1}{\phi^2} \tag{24}$$

For a sandstone:

$$D_e = \frac{0.62}{\phi^{2.15}} \tag{25}$$

The analysis of WK68 was typical and proceeded as follows. A plot similar to Figure 14 was inspected. The breakthrough and peak times were determined visually, in this case 2.3 and 11.09 days. The fracture aperture of 0.0043 in. was then calculated using Equation 20.

Jensen used a nonlinear regression technique. Three parameters were needed to fit the data. α determined the shape of the curve. $1/\beta$ was equal to the breakthrough time, and the third factor was a simple scaling coefficient. The time to peak concentration was not determined explicitly but could be found by manipulating Jensen's equations. For the WK68 Jensen computed a breakthrough time of 2.92 days and a peak time of 11.09 days. The resulting fracture aperture was 0.0068 in., approximately 50 % greater than the width estimated visually. Since both methods were based on the matrix diffusion model, identical picks for the times yielded identical aperture estimates.

Table 3 presents the results of the visual and regression methods. In three cases Jensen found a better match using a double fracture model. Visual analysis of this kind was impossible. When only the ten single fracture fit curves were compared, the estimates of fracture aperture agreed fairly well. Figure 15 shows a plot of width found from the regression and visual procedures. The divergence between the two methods lie within the definitions of accuracy and precision. The average absolute value of the difference between the procedures was 40% (low precision). If the differences are summed while maintaining the positive and negative signs, the average of the discrepancies is only 0.9% (high accuracy).

Figures 16 and 17 attempt to discern the reasons for the discrepancies. The regression method computed both longer breakthrough

Inj. Well	Prod. Well	Regression				Visual			Δb %
		α	$1/\beta$ days	t_p days	b in.	t^* days	t_p days	b in.	
CWK107	WK24	1.25	0.23	0.47	0.0031	0.22	0.51	0.0027	-14
	WK30	1.37	4.37	9.83	0.013	3.7	9.3	0.010	-16
		1.27	3.22	6.67	0.012				-7
	WK48	1.39	0.29	0.67	0.0032	0.26	0.70	0.0026	-17
		1.67	1.04	2.97	0.0050				-48
	WK55	2.58	2.67	14.51	0.0052	3.3	15.7	0.0063	-23
	WK67	2.74	1.65	9.89	0.0038	0.46	15.3	0.0008	-80
	WK68	2.05	2.92	11.09	0.0068	2.3	14.8	0.0043	-35
	WK70	2.48	2.03	10.39	0.0047	2.8	9.9	0.0070	+50
	WK81	1.54	3.66	9.41	0.010	4.0	8.4	0.013	+23
CWK101	WK83	2.17	2.55	10.53	0.0060	3.7	9.7	0.010	+73
	WK108	1.69	6.78	19.62	0.013	10.7	25.6	0.019	+47
	WK103	3.44	0.62	5.49	0.0019	0.54	5.1	0.0017	-10
	WK116	3.84	0.63	6.79	0.0017	2.4	7.0	0.0075	+342
		0.92	4.79	7.35	0.019				-61
	WK121	0.92	1.45	2.26	0.011	1.1	2.5	0.0062	-41

Table 3: Estimation of Fracture Aperture - Regression and Visual Methods

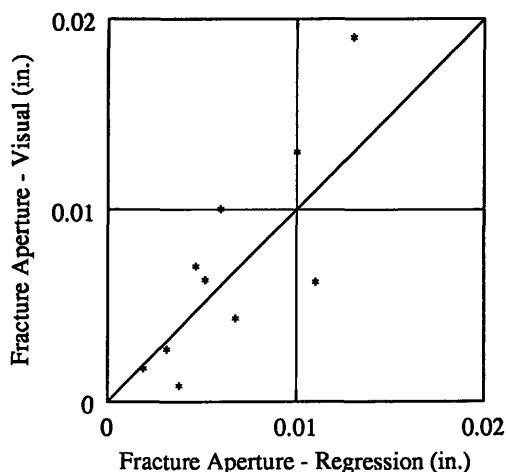


Figure 15: Fracture Aperture - Visual vs. Regression Method

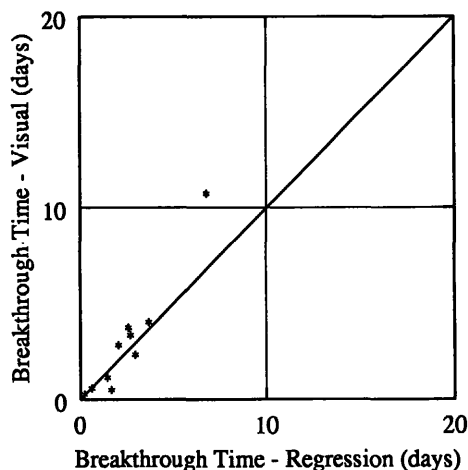


Figure 16: Breakthrough Time - Visual vs. Regression Method

and peak times. Since the difference between the two times is important, the relative overestimation was not the cause of the divergence. The difference was simply a random variation. Perhaps with practice, an engineer could fine tune his judgement.

The visual estimation was probably more accurate in at least one case. In his analysis of the WK116 well (Figure 18), Jensen incorporated data from 0 to 2.4 days. These points included random background radiation. Their inclusion may be the origin of the double fracture fit.

CONCLUSIONS

1. Adsorption is a significant factor in the flow of tracers through fractured rock. This process can occur in two places, on the fissure wall and in the matrix. The effect of areal adsorption is to translate the entire breakthrough curve in time

while adsorption within the rock pores tends to increase dispersion. In the case of a pulsed injection, volumetric adsorption increases the time between breakthrough and the peak concentration. Estimating fracture aperture from tracer tests requires an accurate estimation of the partition coefficients.

2. The fracture aperture may be determined by visually examining tracer breakthrough curves. Accurate estimation of fissure width requires good appraisals of the times to breakthrough and peak concentration. Choosing the correct values of $R_D t^*$ and t_p is not always easy especially when analyzing radioactive tracer data.

ACKNOWLEDGEMENTS

Financial support for this project was provided by the the Department of Energy under Stanford-DOE contract DE-AS07-84ID12529.

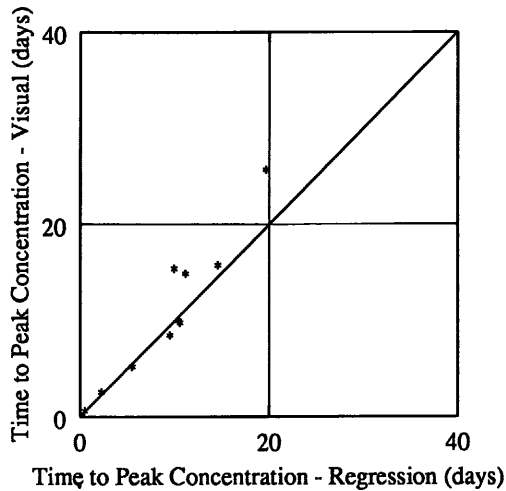


Figure 17: Peak Concentration Time – Visual vs. Regression Method

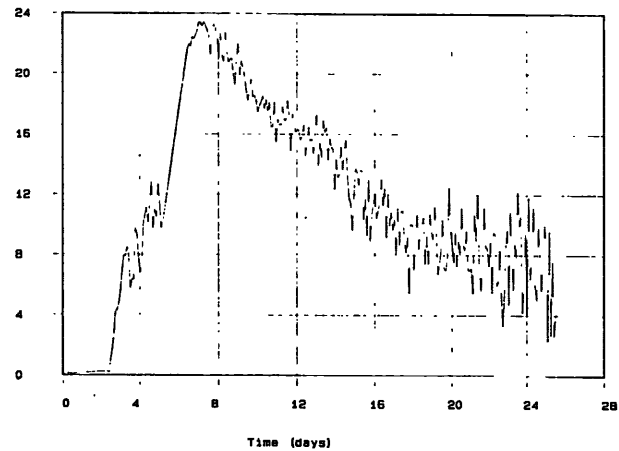


Figure 18: WK116 Tracer Breakthrough Curve – from CWK101

NOMENCLATURE

- A_D dimensionless coefficient
- b fracture aperture, [L]
- b_D dimensionless fracture aperture
- C concentration (mass/volume), [m/L³]
- C_D dimensionless concentration (C/C_0)
- C_f concentration in fracture (mass/liq. vol.), [m/L³]
- C_{fD} dimensionless concentration in fracture (C_f/C_0)
- C_m concentration in matrix (mass/vol. of rock), [m/L³]
- C_p concentration in pores (mass/liq. vol.), [m/L³]
- C_{pD} dimensionless concentration in pores (C_p/C_0)
- C_0 injection or reference concentration, [m/L³]
- C_{fD} dimensionless fracture concentration (C_f/C_0)
- C_1, C_2 constants in conversion of voltage to concentration
- D_a apparent diffusivity ($D_e/(\phi + K_v)$), [L²/t]
- D_D dimensionless diffusivity ($D_e t^*/L^2$)
- D_e effective diffusivity, [L²/t]
- D_0 molecular diffusivity in water, [L²/t]
- F formation factor
- h fracture height, [L]
- K_a areal partition coefficient, [L]
- K_v volumetric partition coefficient, (pore vol/bulk vol)
- $K_d \rho_p$ volumetric equilibrium constant ($\phi + K_v$)
- K_D dimensionless partition coefficient ($\phi + K_v$)
- L fracture length, [L]
- R_D retardation factor ($1 + \frac{2}{\phi} K_a$)
- S concentration of mass adsorbed on rock (mass/rock volume), [m/L³]
- t time, [t]
- t_D dimensionless time (t/t^*)
- t_p time from injection to peak concentration, [t]
- t^* t-star (L/v), [t]
- Δt injection time, [t]
- Δt_D dimensionless injection time ($\Delta t/t^*$)
- v velocity of flow in fracture, [L/t]
- x length along fracture axis, [L]
- x_D dimensionless fracture length
- y distance normal to fracture axis into matrix, [L]
- y_D dimensionless distance into the matrix
- ϕ porosity

REFERENCES

- Carslaw, H. S. and Jaeger, J. C., 1959. Conduction of Heat in Solids. Oxford University Press, New York, Second Edition, p. 396.
- Freeze, R. Allan and Cherry, John A., 1979. Groundwater. Prentice-Hall Inc., Englewood Cliffs, New Jersey, p. 402–413.
- Gray, George R. and Darley, H. C. H., 1980. Composition and Properties of Oil Well Drilling Fluids. Gulf Publishing Company, Houston, Texas, Fourth Edition.
- Grindley, G. W., 1965. The Geology, Structure and Exploitation of the Wairakei Geothermal, Taupo, New Zealand. New Zealand Geological Society Bulletin, v. 75, p. 104.
- Jensen, Clair L., 1965. Matrix Diffusion and Its Effects on the Modeling of Tracer Returns from the Fractured Geothermal Reservoir at Wairakei, New Zealand. Technical Report SGP-TR-71, Stanford Geothermal Program.
- McCabe, W. J., Barry, B. J. and Manning M. R., 1983. Radioactive Tracers in Geothermal Underground Water Flow Studies. Geothermics, v. 12, p. 83–110.
- Neretnieks, Ivars, 1980. Diffusion in the Rock Matrix: An Important Factor in Radionuclide Retardation? Jour. of Geophys. Res. v. 85 p. 4379–4397.
- Perkins, T. K. and Johnston, O. C., 1963. A Review of Diffusion and Dispersion in Porous Media. Soc. of Pet. Eng. Jour., March.
- Skagius, K., Svedberg, G. and Neretnieks, I., 1982. A Study of Strontium and Cesium Sorption on Granite. Nuclear Technology, v. 59, p. 302–313.
- Taylor, Sir Geoffrey F.R.S., 1953. Dispersion of Soluble Matter in Solvent Flowing Slowly through a Tube. Proceedings of the Royal Society of London, v. 219 p. 186–203.